

Reaction Behavior of Mixtures of Non-Corrosive Flux and Non-Corrosive Flux Containing Zn during Brazing*

Hidetoshi Kumagai** and Naoki Yamashita**

The reaction behaviors of a non-corrosive flux (the NC-flux), non-corrosive flux containing Zn (KZnF₃) and their mixture during brazing were investigated. Regarding the mixture of the NC-flux and KZnF₃, a behavior different from the single-component flux was observed. KZnF₃ in the flux mixture was completely consumed above 500°C, and pure Zn was detected at 500°C. It was considered that this behavior of the flux mixture was due to the reactions of KZnF₃ with Al₂O₃ and the reduction of ZnO by KAlF₄.

Keywords: aluminum brazing, non-corrosive flux, chemical reactions

1. Introduction

Aluminum automotive heat exchangers are generally manufactured by controlled atmosphere brazing (CAB) using a non-corrosive flux (the NC-flux), such as the potassium aluminum fluorides of KAlF₄, K₂AlF₅ and K₃AlF₆. Recently, a non-corrosive flux containing Zn (the Zn-flux), such as the potassium zinc fluoride of KZnF₃ is also being widely used. The significant feature of the Zn-flux is that the Zn diffusion layer into the aluminum multi-port extrusion tube is for protection from the corrosion perforation formed during brazing. Therefore, the application of this flux removes the requirement of the conventional process of Zn arc spraying onto the aluminum multi-port extrusion tube, and also reduces the manufacturing cost. Furthermore, it also allows applying the mixture of both the NC-flux and the Zn-flux.

The reactions of the Zn-flux versus the oxygen concentration and the moisture during brazing are more sensitive than those of the NC-flux. Therefore, it is difficult to make good brazing joints without defects like discoloration by applying the Zn-flux. Since the mechanism of the reactions of the Zn-flux

has not been widely reported, this paper describes the reaction mechanism of the NC-flux, the Zn-flux and their mixture during brazing.

2. Experimental Procedure

2.1 Brazing of single substance and mixture of fluxes

Table 1 shows the specimens, and **Fig. 1** shows the relationship between the oxygen concentration in a furnace and the material temperature during brazing. KZnF₃ was added and mixed with the NC-flux at 0%, 50% and 100% fractions. These fluxes were dispersed in an organic solvent, then brushed on 3003 alloy sheets (25 mm × 25 mm, O temper). After drying, these were brazed at the maximum temperature of 400°C, 500°C and 600°C in the brazing furnace with

Table 1 Specimens for brazing and XRD analysis. (mg)

Sample name	Amount of flux		
	NC-flux (KAlF ₄)	KZnF ₃	Total
Z0	4	0	4
Z100	0	4	4
Z50	2	2	4

* The main part of this paper was published in the proceedings of the 12th Vehicle Thermal Management systems (VTMS12), England, May, 10-13, 2015.

** No. 4 Research Department, Research & Development Division, UACJ Corporation

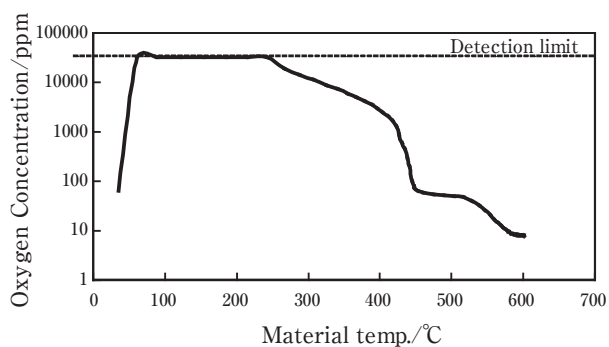


Fig. 1 Relationship between oxygen concentration in furnace and material temperature during brazing.

N_2 atmosphere. The oxygen concentration in the brazing furnace is over 2500 ppm below 400°C, 50-2500 ppm in the range of 400-500°C, and below 50 ppm in the range of 500-600°C. The specimens after brazing were analyzed by X-ray diffraction (XRD). Regarding the Z50 brazed at 500°C, observations by scanning electron microscopy (SEM) and elemental analysis by energy dispersive X-ray spectrometry (EDX) were carried out.

2.2 Additional examinations

2.2.1 Validation of chemical reactions

Table 2 shows the specimens for thermogravimetric and the differential thermal analysis (TG-DTA) and XRD analysis. The after estimated chemical reactions could be validated by TG-DTA. The specimens in the Pt pan were heated at the rate of 20°C/min and the flow rate of the argon gas or the air was 300 ml/min. All of the specimens were analyzed by TG-DTA. P1, P2 and P3 were analyzed by the XRD after the TG-DTA.

2.2.2 Further validation for reduction of ZnO

Regarding the reduction of ZnO, a further validation was determined. The mixture of the

Table 2 Specimens for TG-DTA and XRD analysis.

Sample name	Blend ratio (%)				Flow gas species
	NC-flux (KAlF ₄)	KZnF ₃	Al ₂ O ₃	ZnO	
P1	-	50	50	-	Atmospheric air
P2	-	100	-	-	Ar
P3	50	-	-	50	Ar
KZnF ₃	-	100	-	-	Ar
NC-flux	100	-	-	-	Ar

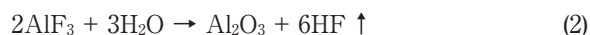
NC-flux and ZnO (75:25) was brazed at the maximum temperature of 600°C. The mixture of approx. 2.7 mg was dispersed in an organic solvent and dropped onto the center of the A3003 alloy sheet (50 mm × 50 mm, O temper). After drying, the specimen was brazed under the same condition as **2.1**. The specimen after brazing was analyzed by the XRD.

3. Results and Discussion

3.1 Brazing of single substance and mixture of flux

3.1.1 Z0 (NC-flux: 100%, KZnF₃: 0%)

Fig. 2 shows the appearance of the specimens after brazing and **Fig. 3** shows the XRD patterns of Z0 after brazing. At the maximum temperature of both 400°C and 500°C, the appearance of the specimen after brazing had a white color and powdery that was the same as the specimen before brazing. In the XRD patterns, KAlF₄ and K₃AlF₆ were detected. At the maximum temperature of 600°C the appearance of the specimen had a transparent color and melt-solidified. It was considered that the flux had normally melted. In the XRD patterns, KAlF₄ and K₃AlF₆ were detected. The intensity of the diffraction peaks for K₃AlF₆ increased with the elevating maximum temperature of brazing. The reason why K₃AlF₆ was detected at such the low temperature of 400°C was considered to be due to the oxygen concentration below 500°C during brazing being high, i. e., 50-2500 ppm or more. It means that the atmosphere in the brazing furnace contained not only O₂, but also H₂O. Therefore, KAlF₄ brazed in a bad atmosphere reacted with H₂O to form K₃AlF₆ following the chemical reaction equations (1)-(3)^{1),2)}.



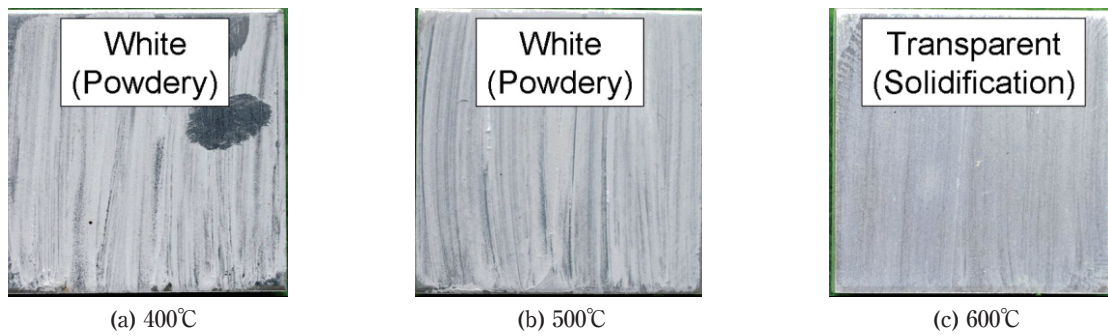


Fig. 2 Appearance of Z0 after brazing at various temperatures.

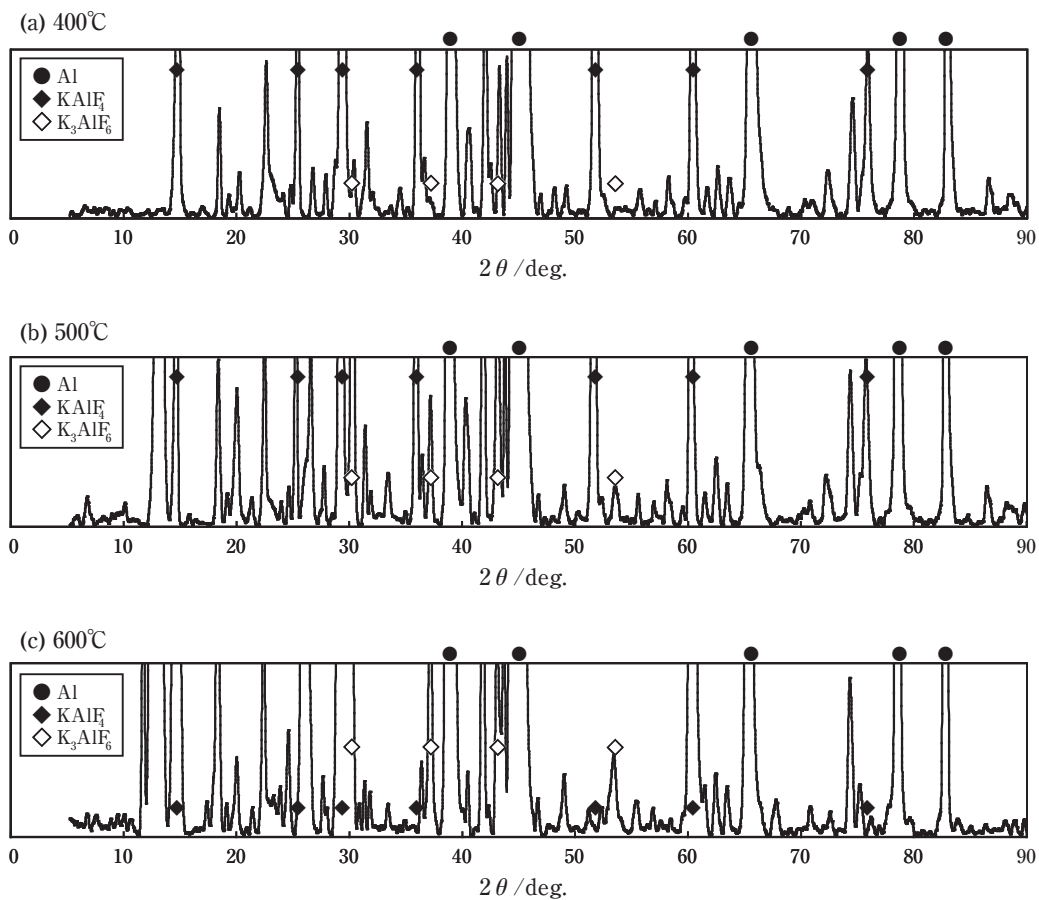


Fig. 3 XRD patterns of Z0 after brazing at various temperatures.

3.1.2 Z100 (NC-flux: 0%, KZnF₃: 100%)

Fig. 4 shows the appearance of the specimens after brazing and Fig. 5 shows the XRD patterns of Z100 after brazing. At the maximum temperature of 400°C, the appearance of the specimen after brazing had a white color and powdery that was the same as the specimen before brazing. In the XRD patterns, KZnF₃ and slight almost of ZnO were detected. At the maximum temperature of 500°C, the appearance of the specimen had a white color and powdery. In the

XRD patterns, KZnF₃, K₃AlF₆ and ZnO were detected. At the maximum temperature of 600°C, the appearance of the specimen had a transparent color and melt-solidified as well as Z0. It was considered that the flux had normally melted. In the XRD patterns, KAlF₄ and K₃AlF₆ were detected, but KZnF₃ and ZnO were not detected. KZnF₃ generally reacts with the aluminum at approx. 555°C following the chemical reaction equation (4) to form KAlF₄, K₃AlF₆ and Zn³.

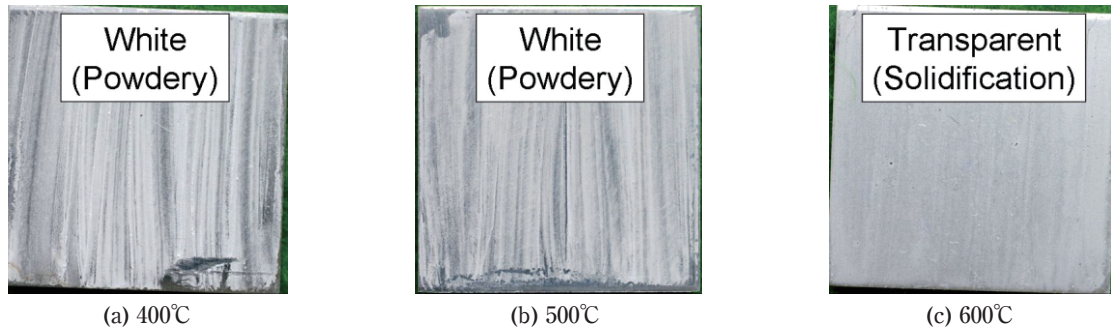


Fig. 4 Appearance of Z100 after brazing at various temperatures.

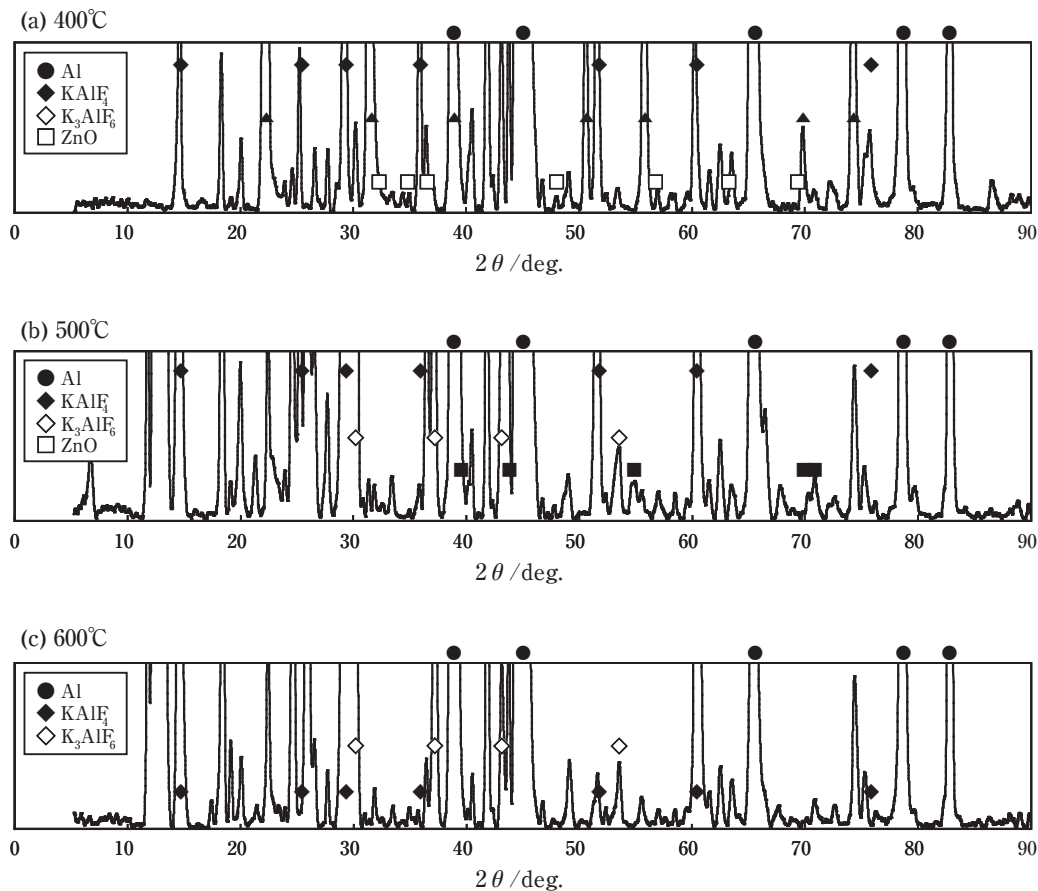
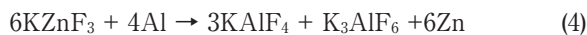


Fig. 5 XRD patterns of Z100 after brazing at various temperatures.

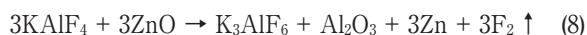


Below 500 °C, however, eq. (4) could not occur. Therefore, it was estimated that chemical reaction equations (5)-(7) could occur.



Eq. (5) is the reaction of KZnF_3 with the oxide film on the aluminum, and eq. (7) is the reaction of KZnF_3 with H_2O in the brazing atmosphere. Although the amount of K_3AlF_6 was too low to detect in the XRD patterns at the maximum temperature of 400°C, it was considered that KAlF_4 formed by eq. (5) reacted with KF formed by eqs. (1) and (6) to form K_3AlF_6 as well as ZnO . It was considered that most of the KZnF_3 not in contact with the surface of the aluminum base

material could not have reacted and therefore remained, because eq. (5) occurred on the surface of the aluminum base material. Furthermore, it was considered that eqs. (6) and (7) also occurred on the $KZnF_3$. However, ZnO was not detected at $600^\circ C$. It was considered that the following chemical reaction equation (8) could occur.



Above $500^\circ C$, eq. (4) occurred at approx. $555^\circ C$, i. e., the formed $KAlF_4$ and K_3AlF_6 were melted at approx. $562^\circ C$. Finally, Zn diffused into the aluminum base material.

3.1.3 Z50 (NC-flux: 50%, $KZnF_3$: 50%)

Fig. 6 shows the appearance of the specimens after brazing, **Fig. 7** shows the XRD patterns of Z50 after brazing and **Fig. 8** shows the SEM image and EDX analysis at the maximum temperature of $500^\circ C$. At the maximum temperature of $400^\circ C$, the appearance

of the specimen after brazing had a white color and powdery that was the same as the specimen before brazing. In the XRD patterns, $KAlF_4$, $KZnF_3$ and a slight ZnO were detected. At the maximum temperature of $500^\circ C$, the appearance of the specimen had a slight gray color and powdery. In the XRD patterns, $KAlF_4$, K_3AlF_6 and Zn were detected, but $KZnF_3$ and ZnO were not detected. At the maximum temperature of $600^\circ C$, the specimen had a transparent color and melt-solidified as well as Z0 and Z100. It was considered that the flux had normally melted. Below $400^\circ C$, it was considered that chemical reactions, eqs. (1)-(3) and (5)-(7), occurred as well as Z100. At the maximum temperature of $500^\circ C$, ZnO was not detected in the XRD patterns and spherical Zn was observed by the SEM and the EDX analysis. The shape of the spherical Zn indicates that there was melted Zn . Therefore, it was considered that eq. (8) occurred. On the other hand, as the reason why $KZnF_3$ was completely consumed at $500^\circ C$, it was considered that eqs. (5)-(8) occurred. First, eqs. (6) and (7) occurred and

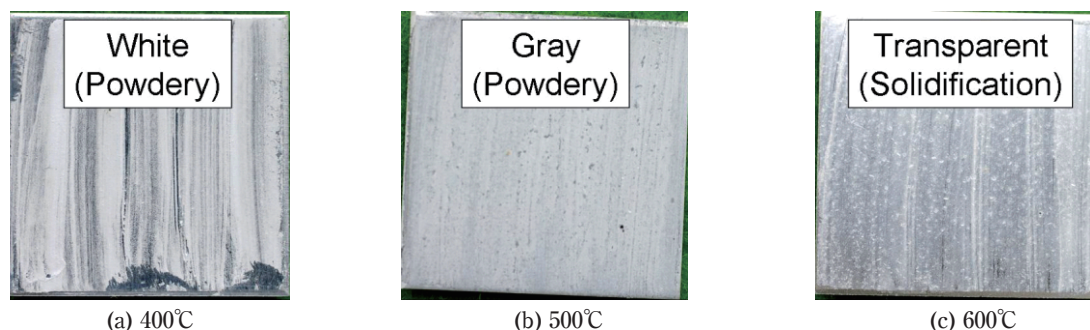


Fig. 6 Appearance of Z50 after brazing at various temperatures.

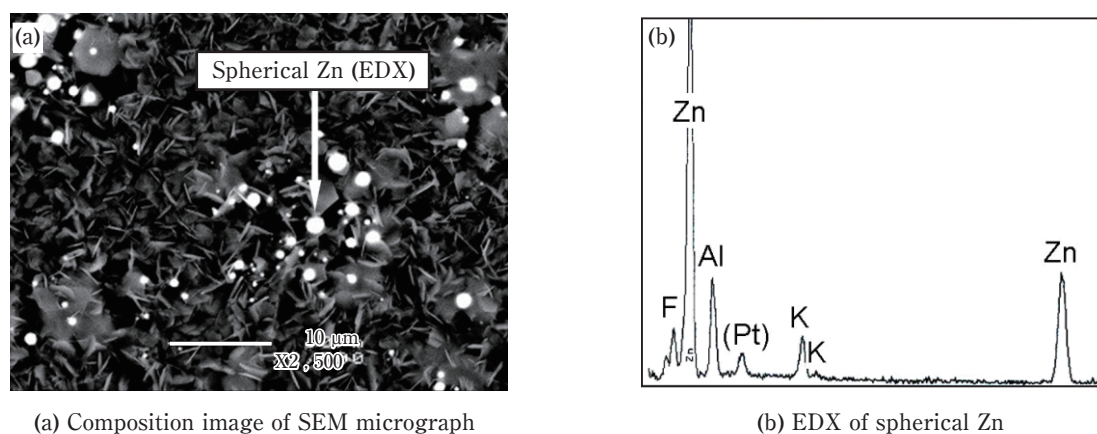


Fig. 7 SEM micrograph and EDX of Z50 after brazing at $500^\circ C$.

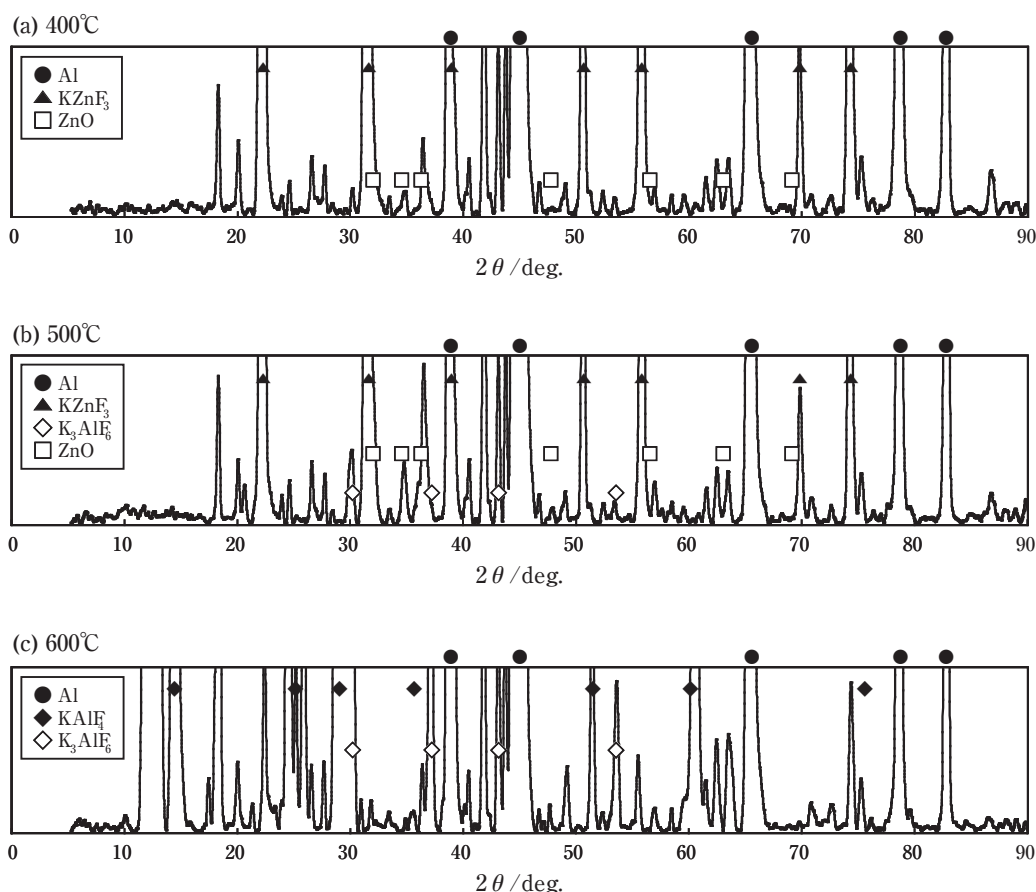


Fig. 8 XRD patterns of Z100 after brazing at various temperatures.

ZnO was formed in all over Z50, then eq. (8) occurred in Z50 as the reaction between ZnO formed by eqs. (6) and (7) and KAlF_4 because KAlF_4 was included in Z50 as one of the components before brazing. Furthermore, eq. (5) occurred as the reaction between KZnF_3 and Al_2O_3 of both the oxide film and the product by eq. (8), then both eqs. (5) and (8) continuously occurred by means of the product of each equation as the reactant of the each equation respectively. Consequently, KZnF_3 had been completely consumed. As the reason why the spherical Zn was observed at 500°C, it was inferred that KAlF_4 and K_3AlF_6 prevented Zn diffused to the base material. Below 562°C, the unmelted KAlF_4 and K_3AlF_6 prevented Zn from diffusing into the aluminum base material, therefore, the melted Zn was spherically agglomerated. At the maximum temperature of 600°C, KAlF_4 and K_3AlF_6 had already melted. Therefore, Zn diffused into the aluminum base material.

3.2 Additional examination – Validation of chemical reactions

3.2.1 P1 (KZnF_3 : 50%, Al_2O_3 : 50%, Flow gas: Ar)

Fig. 9 shows the TG-DTA curves of P1 and KZnF_3 and Fig. 10 shows the XRD patterns of P1 after the TG-DTA. For the validation of eq. (5), KZnF_3 and Al_2O_3 were mixed and heated in the flowing argon gas at the maximum temperatures of 388°C, 492°C, 593°C and 638°C. A clear endothermic peak was observed at around 628°C in the DTA curve of P1, and the weight loss started shortly after the onset of heating in the TG curve of both P1 and KZnF_3 . In the TG curves, the starting temperature of the weight loss of P1 was equal to that of KZnF_3 . Therefore, it was considered that the weight loss of P1 originated in KZnF_3 as a component of P1. However, the cause of the weight loss at such a low temperature was unclear. In the XRD patterns at the maximum temperature of 388°C and 492°C, KZnF_3 , Al_2O_3 and ZnO were detected, and at the maximum temperature or 593°C, KZnF_3 , K_3AlF_6 , Al_2O_3 and ZnO

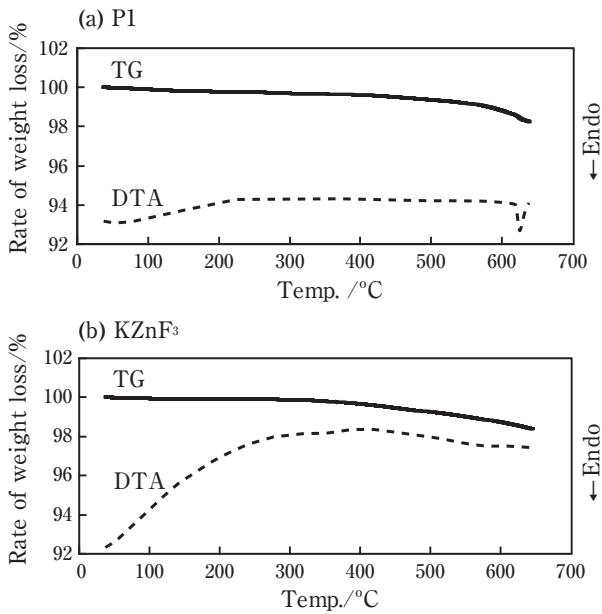


Fig. 9 Results of TG-DTA for P1 and KZnF₃.

were detected. Furthermore, at the maximum temperature of 638°C, KAlF₄, K₃AlF₆, Al₂O₃ and ZnO were detected whereas KZnF₃ was not detected. Based on these results, it was considered that KZnF₃ reacted with Al₂O₃ based on eq. (5) was below 400°C, and it was considered that the reaction of eq. (5) completed at approx. 600°C.

As for the reason why KAlF₄ was not detected after heating, it was considered that eq. (8) occurred in parallel with eq. (5) by KAlF₄ and ZnO being produced by eq. (5), consequently KAlF₄ was consumed. Furthermore, as for the reason why K₃AlF₆ was not detected at 388°C and 492°C, it was considered that the amount of K₃AlF₆ as the product below 500°C was too low to detect. However, the reason why Zn produced by eq. (8) was not detected is still unclear.

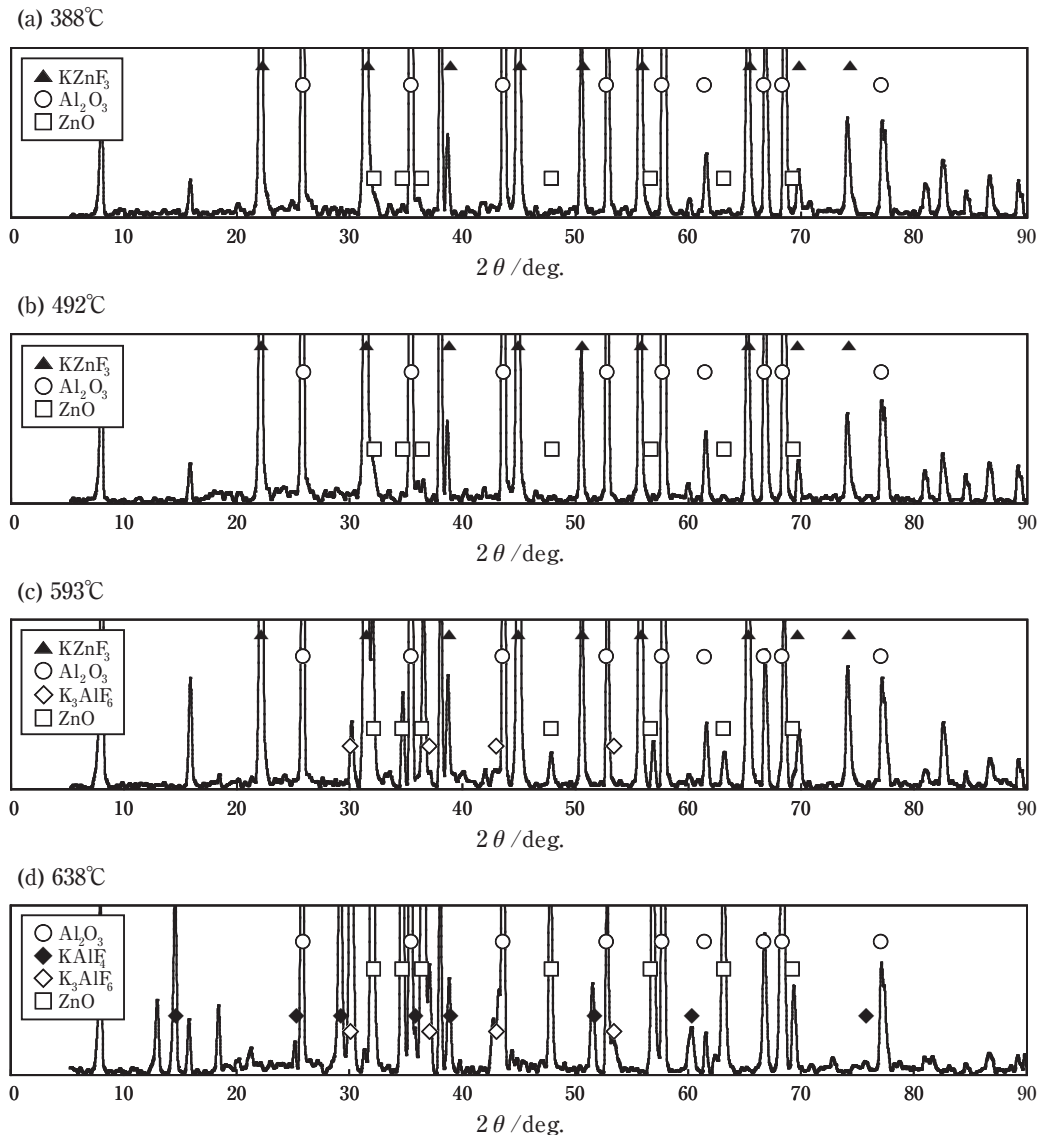


Fig. 10 XRD patterns of P1 after TG-DTA.

3.2.2 P2 (KZnF₃: 100%, Flow gas: Atmospheric air)

Fig. 11 shows the results of the TG-DTA and Fig. 12 shows the XRD patterns of P2 after the TG-DTA. For the validation of eqs. (6) and (7), KZnF₃ was heated in flowing air at the maximum

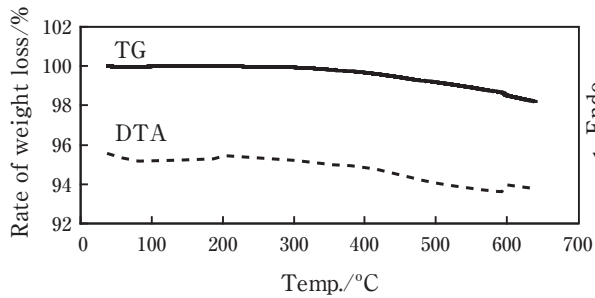
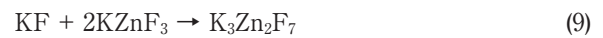


Fig. 11 Results of TG-DTA for P2.

temperatures of 388°C, 492°C, 593°C and 639°C. A slight exothermic peak was observed at approx. 600°C in the DTA curve, and the weight loss started at approx. 280°C in the TG curve. It was similar to the result of Fig. 9. In the XRD patterns, KZnF₃ and ZnO were detected at the maximum temperature of 388°C, 492°C and 593°C. KZnF₃, K₃Zn₂F₇ and ZnO were detected at the maximum temperature of 639°C. Therefore, in the case of heating KZnF₃ in a high concentration of O₂ and H₂O, it was considered that the reaction occurred not only by eqs. (6) and (7) but also by eq. (9). Especially, eq. (9) occurred at approx. 600°C.



Therefore, eq. (6) and (7) were validated.

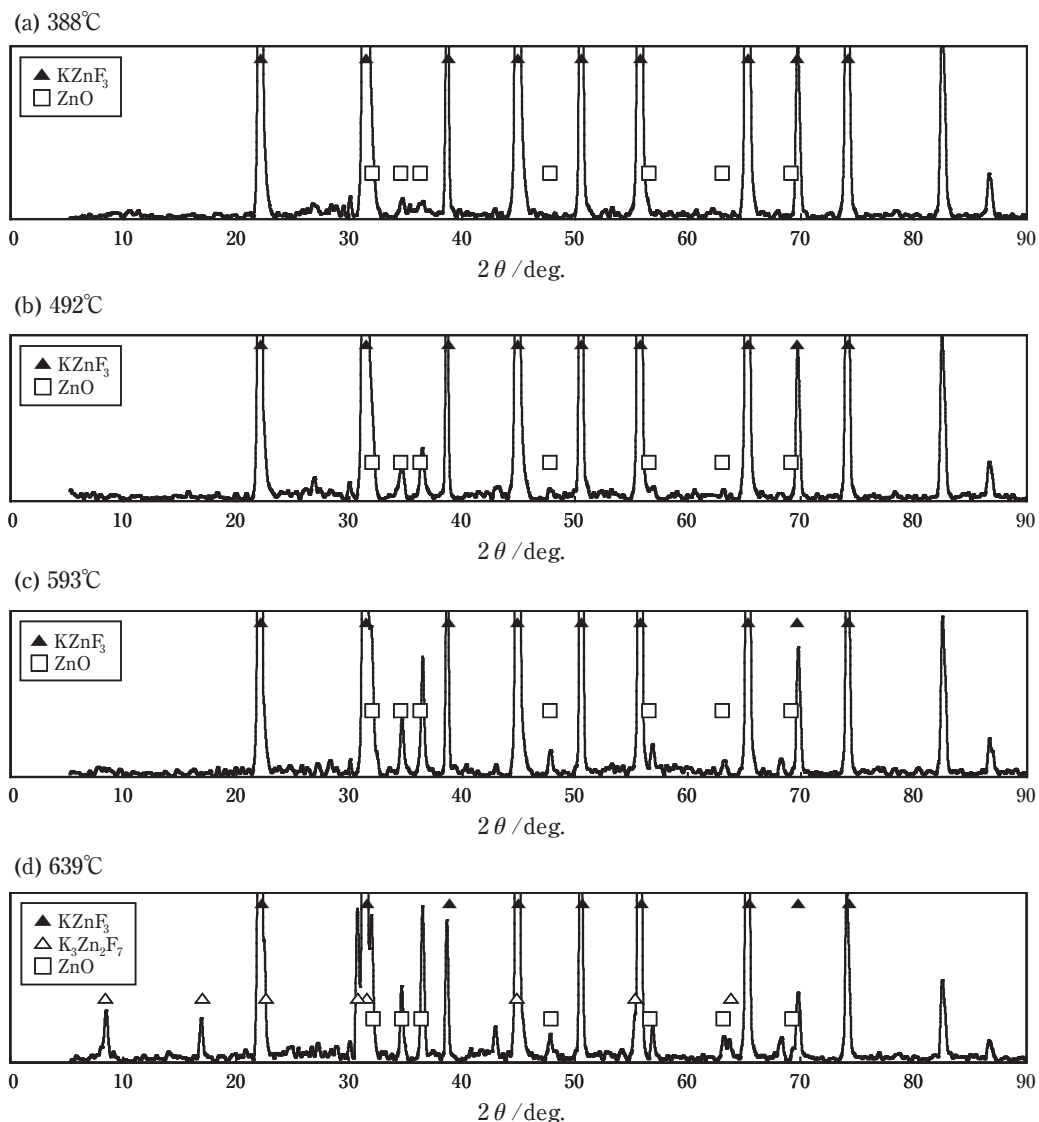


Fig. 12 XRD patterns of P2 after TG-DTA

3.2.3 P3 (NC-flux: 50%, ZnO: 50%, Flow gas: Ar)

Fig. 13 shows the TG-DTA curves of P3 and the NC-flux and **Fig. 14** shows the XRD patterns of P3 after the TG-DTA. For the validation of eq. (8), the NC-flux and ZnO were mixed and heated in flowing argon gas at the maximum temperatures of 385°C, 489°C, 589°C and 638°C. Clear endothermic peaks were observed at approx. 100°C and approx. 560°C in the DTA curve of both P3 and the NC-flux. A clear weight loss was observed at approx. 100°C and above approx. 380°C and approx. 550°C in the TG curve of both P3 and the NC-flux. As for the reason why the endothermic peak and the weight loss were observed at approx. 100°C, it was considered to be due to the vaporization of the hydrated water in the NC-flux. As for the reason why the endothermic peak and the

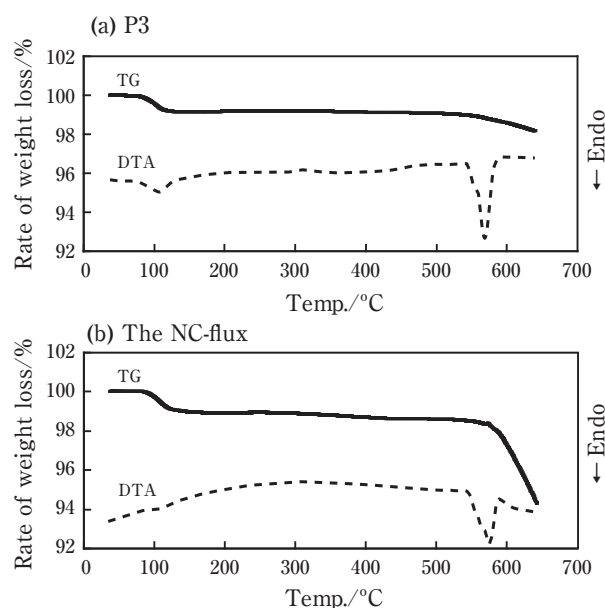


Fig. 13 Results of TG-DTA for P3 and the NC-flux.

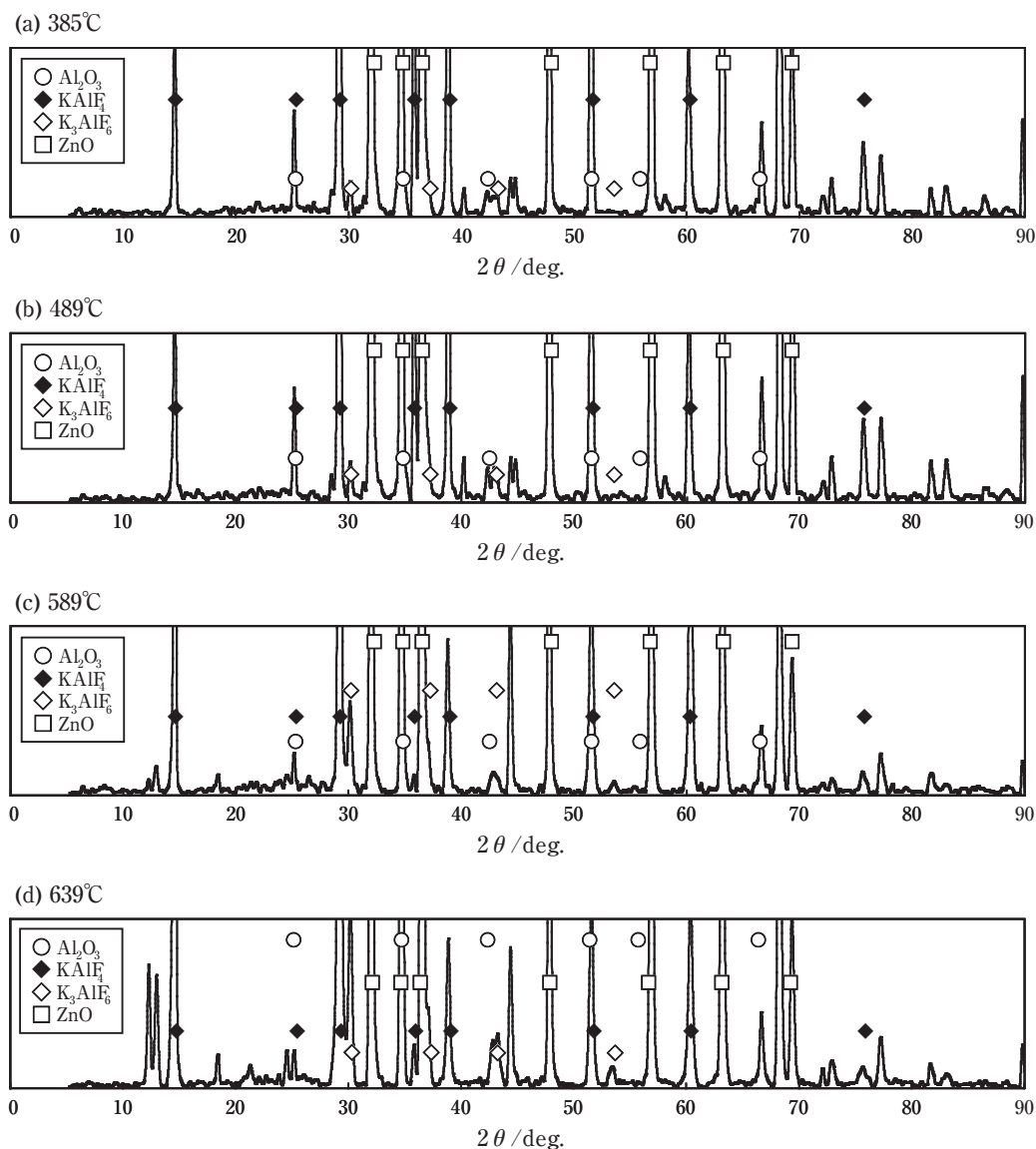


Fig. 14 XRD patterns of P3 after TG-DTA.

weight loss were observed at approx. 560°C, it was considered to be the melting point of $KAlF_4$. In addition, for the relatively slight weight loss observed above approx. 380°C, it was considered that this weight loss indicated the emission of F gas and the vaporization of $KAlF_4$ ²⁾. The weight loss due to the vaporization of $KAlF_4$ was especially prominent above approx. 550°C, close to the temperature near the melting point of $KAlF_4$. In the XRD patterns, $KAlF_4$, K_3AlF_6 , Al_2O_3 and ZnO were detected. Therefore, it was considered that eq. (8) occurred at approx. 380°C based on the weight loss at approx. 380°C. However, the reason why Zn produced by eq. (8) was not detected is unclear. For further validation in regard to the formation of Zn, it means the reduction of ZnO, and the additional brazing test shown in the next section.

3.3 Additional examination - Further validation for reduction of ZnO

Fig. 15 shows the appearance of the mixture of the NC-flux and ZnO after brazing and **Fig. 16** shows the XRD patterns of the mixture after brazing. For further validation of eq. (8), the center of the dropped

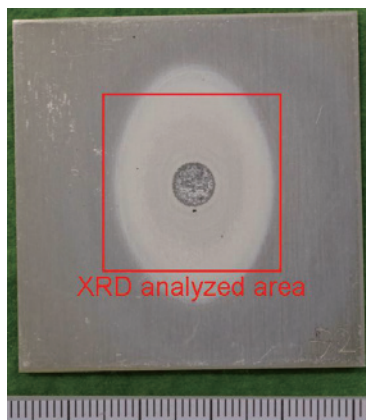


Fig. 15 Appearance of the NC-flux+ZnO after brazing.

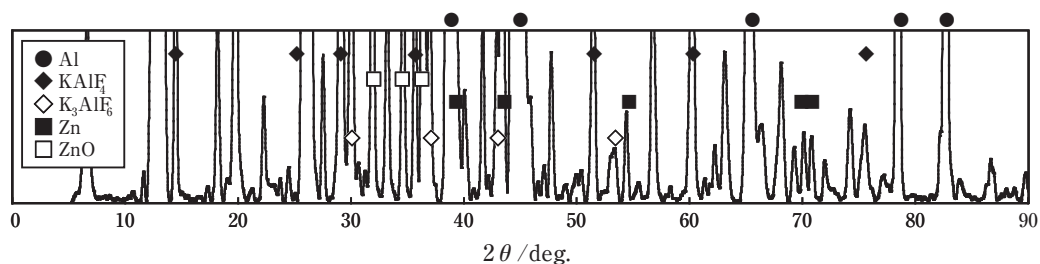


Fig. 16 XRD patterns of the NC-flux+ZnO after brazing.

flux on the 3003 alloy sheet (25 mm × 25 mm) after brazing was analyzed by XRD. The black residue was observed on the dropped position of the specimens after brazing. In the XRD patterns, $KAlF_4$, K_3AlF_6 , Zn and ZnO were detected. It was considered that the black residue was the agglomerated Zn shown in Fig. 7, because K_3AlF_6 prevented the Zn from diffusing into the aluminum base material. Therefore, eq. (8) was validated. However, the reason why Zn was not detected on P3 specimens after the TG-DTA whereas Zn was detected after this brazing test is still unclear. This reason was inferred that a produced Zn could not be detected by the XRD because of very slight, or a produced Zn was vaporized. Therefore, the condition of the TG-DTA is needed to rethink.

4. Conclusion

The reaction behavior of the NC-flux, $KZnF_3$ and their mixture during brazing were investigated.

- (1) Regarding the NC-flux, K_3AlF_6 increased with the elevating temperature increase during brazing.
- (2) Regarding $KZnF_3$, $KZnF_3$ reacted with the oxide film on the aluminum base material and H_2O in the brazing atmosphere, subsequently ZnO was formed below 500°C. Finally, Zn was formed due to the reduction of ZnO by $KAlF_4$.
- (3) Regarding the mixture of the NC-flux and $KZnF_3$, $KZnF_3$ reacted with the oxide film on the aluminum base material and H_2O in the brazing atmosphere, then ZnO was formed below 400°C. In the temperature range of 400–500°C, Zn and Al_2O_3 were formed from the reductive reaction of ZnO by $KAlF_4$. These reactions occurred not only at the surface of

the aluminum base material but also all over the specimen. Furthermore, the Al_2O_3 formed by this reaction was used as the source of the reaction with KZnF_3 . Consequently, KZnF_3 was completely consumed in the range of 400-500°C. Finally, Zn was formed due to the reduction of ZnO by KAlF_4 .

References

- 1) W. T. Thompson and D. W. G. Goad: Can. J. Chem., **54** (1976), 3342-3349.
- 2) T. Takemoto, A. Matsunawa and A. Kitagawa: Journal of Materials Science Letters, **15** (1996), 301-303.
- 3) P.G.Juan, H. W. Swidersky, T. Schwarze and J. Eicher: "Functionalized Inorganic Fluorides: Synthesis, Characterization and Properties of Nanostructured Solides (Ed. A. Tressud), Chapter 7. Inorganic Fluoride Materials from Solvay Fluor and their Industrial Applications", (2010), 210-211, Jhon & Sons, Ltd., Chichester, UK., doi: 10.1002/9780470660768.ch7.



Hidetoshi Kumagai

No. 4 Research Department, Research & Development Division, UACJ Corporation



Naoki Yamashita

No. 4 Research Department, Research & Development Division, UACJ Corporation